

SECOND ORDER NLO, THIRD ORDER NLO AND DIELECTRIC STUDIES OF LITHIUM SULFATE CRYSTALS DOPED WITH RUBIDIUM CHLORIDE

P. Manimekalai* & P. Selvarajan**

* Department of Physics, Christ the King Polytechnic College, Othakkalmandapam, Coimbatore, Tamilnadu

** Department of Physics, Aditanar College of Arts and Science, Tiruchendur, Tamilnadu

Cite This Article: P. Manimekalai & P. Selvarajan, "Second Order NLO, Third Order NLO and Dielectric Studies of Lithium Sulfate Crystals Doped with Rubidium Chloride", International Journal of Advanced Trends in Engineering and Technology, Volume 3, Issue 1, Page Number 63-69, 2018.

Abstract.

Single crystals of undoped and rubidium chloride doped lithium sulfate were grown by solution method with slow evaporation technique. The reactants used are AR grade lithium sulfate and rubidium chloride and double distilled water was used as the solvent. Colourless, transparent and non-hygroscopic crystals were harvested after a growth period of 35 days. The crystal structure was found by XRD studies. Second order NLO studies were carried out by Kurtz-Perry powder technique. Third order NLO studies were done on the grown crystals by Z-scan technique and nonlinear optical refractive index, nonlinear absorption coefficient and nonlinear susceptibility were determined. The dielectric constant and dielectric loss of the samples have been found at different frequencies and temperatures and the results are discussed.

Key Words: Lithium Sulfate, Doping, Solution Growth, XRD, SHG, Z-Scan Technique, Dielectric Constant, Nonlinear Refractive Index & Nonlinear Susceptibility

1. Introduction:

The design of optoelectronics and photonic devices realizes heavily in the development of nonlinear optical materials with higher efficiency. So the materials possessing large second order nonlinear susceptibility with favorable in thermal and mechanical stability are intensively used in many device applications [1-3]. Complex of sulfates are of great interest in industry, due to their outstanding physical properties and widely used as nonlinear optical (NLO), ceramic, ferroelectric, electric, and catalytic materials [4-7]. Lithium sulfate is one of the sulfates and it crystallizes in P2₁ space group with monoclinic structure. The structural analysis of lithium sulfate crystal was already reported [8, 9]. Many researchers studied on various properties of lithium sulfate crystals and reported in the literature [10-15]. In this work, single crystals of undoped and rubidium chloride doped lithium sulfate (RCLS) crystals have been grown by the slow evaporation technique. The grown crystals were characterized by XRD studies, second order NLO studies, third order NLO studies and dielectric studies.

2. Preparation of Samples:

Commercially available AR grade lithium sulfate and rubidium chloride were used as the reactant materials for the growth of undoped and rubidium chloride doped lithium sulfate crystals. Saturated solution of lithium sulfate was prepared using the double distilled water as the solvent and it was stirred well with a magnetic stirrer for about 2 hours. Then it was filtered into the growth vessel using the Whatmann filter papers. The growth vessel was covered with a perforated cover for occurring slow evaporation. Due to slow evaporation, single crystals of undoped lithium sulfate were grown after growth period of 25 days. Rubidium chloride doped lithium sulfate crystals were grown by taking lithium sulfate and rubidium chloride in molar ratio of 1:0.01. Using double distilled water as the solvent, saturated solution was prepared, stirred and filtered. Due to slow evaporation, single crystals of the doped lithium sulfate were grown. It is to be mentioned here that the saturated solution was initially converted into supersaturated solution due to slow evaporation and the growth process has be started. The harvested crystals of undoped and rubidium chloride doped crystals are shown elsewhere [15].

3. Finding Crystal Structure:

X-ray diffraction (XRD) is an important method for finding the crystal structure of the grown crystals. The condition for XRD is the Bragg's law and it is given by $n\lambda=2d\sin\theta$ and this law relates the wavelength of electromagnetic radiation (λ), the Bragg's angle (θ) and the interplaner spacing (d). Using the computerized single crystal X-ray diffractometer, the lattice parameters of the samples are obtained. Here a Bruker-Nonius MACH3/CAD4 single crystal X-ray diffractometer with MoK $_{\alpha}$ radiation (λ =0.71069 Å) was used collect the XRD data of the samples. The obtained single crystal XRD data for undoped lithium sulfate crystal are a = 5.478(4) Å, b = 4.875(2) Å, c = 8.179(3) Å and $\alpha = \gamma = 90^{\circ}$, $\beta = 106.98(5)$. The XRD data obtained for rubidium chloride doped lithium crystal are a = 5.527 (3) Å, b = 4.892(2) Å, c = 8.187 (6) Å and $\alpha = \gamma = 90^{\circ}$, $\beta = 106.25(5)$ and the results indicate that the grown crystals are found to be crystallizing in monoclinic structure.

4. Second Order NLO Studies: Second order nonlinear optical effects are second harmonic generation, sum frequency generation, different frequency generation, optical rectification etc. Second harmonic generation

(SHG) is a nonlinear optical process that results in the conversion of an input optical wave into an output wave

of twice the input frequency. The process of second harmonic generation by an incident wave of frequency ω_1 is a two step process. In the first step, a polarization wave at the second harmonic frequency 2ω, is produced which has a phase velocity and wavelength in the medium which are determined by the refractive index of the fundamental wave (n₁). The second step is the transfer of energy from the polarization wave to an electromagnetic wave at frequency $2\omega_1$. The phase velocity and the wavelength of this electromagnetic wave are determined by n₂, the refractive index of the doubled frequency. For efficient energy transfer it is essential that the two waves remain in phase, which means that $n_1 = n_2$ Since almost all materials have normal dispersion in the optical region, the radiation will generally lag behind the polarization wave, which leads to a phase mismatch. The second harmonic power generation is strongly dependent on the phase mismatch produced. An effective method of providing equal phase velocities for the fundamental and second harmonic waves in the nonlinear medium utilizes the fact that dispersion can be offset by using the natural birefringence of nonlinear optical uniaxial or biaxial crystals. Here the relative SHG efficiency of the samples was measured using Kurtz and Perry powder technique [16]. Second harmonic generation efficiency of grown crystal lithium sulfate monohydrate crystal was estimated by Kurtz and Perry powder technique with the help of Nd:YAG laser beam of wavelength 1064 nm. The grown crystal was powdered to the particle size in the range 125-150 µm. The crystal was densely packed in a micro capillary tube. The first harmonic output of 1064 nm from Nd:YAG laser was made to fall normally on the sample. The SHG behavior of the crystal was confirmed from the emission of intense green radiation ($\lambda = 532$ nm). The SHG efficiency of undoped lithium sulfate monohydrate crystal was found to be 0.97 times that of KDP crystal. Similarly, the SHG efficiency of rubidium chloride doped lithium sulfate sample was found to be 1.26 times that of the reference sample KDP sample. Secondharmonic generation is used often in devices where photons of visible frequency are desired but the available underlying laser system is capable of producing only infrared photons.

5. Third Order NLO studies:

Third-order nonlinear optical (NLO) parameters such as nonlinear refractive index (n₂), nonlinear susceptibility and nonlinear absorption coefficient (β) have been determined using the Z-scan technique [17, 18]. Normalized transmittance was measured by varying the sample position (Z) in open and closed aperture modes. Using the closed aperture curve, the thirdorder nonlinear refractive index (n_2) can be found and using the open aperture curve, the nonlinear absorption coefficient (β) and third order susceptibility can be found. In the closed aperture method, an aperture is placed to prevent some of the light from reaching the detector. A lens focuses a laser to a certain point, and after this point the beam naturally defocuses. After a further distance an aperture is placed with a detector behind it. The aperture causes only the central region of the cone of light to reach the detector. The detector is sensitive to any focusing or defocusing that a sample may induce. The sample is typically placed at the focus point of the lens, and then moved along the Z-axis. Open aperture method is similar to the above method, however the aperture is removed or enlarged to allow all the light to reach the detector. This is used in order to measure the nonlinear absorption coefficient. The laser light intensities, transmitted across the sample, are measured as a function of sample position in the Z-direction with respect to the focal plane either through a closed aperture (CA) or open aperture (OA) in order to resolve the nonlinear refraction and absorption coefficients. For an open aperture Z-scan, a lens replaces the aperture to collect the entire laser beam transmitted through the sample. The study of nonlinear refraction by the Z-scan method depends on the position (Z) of the thin sample under the investigation along a focused Gaussian laser beam. The Z-scan curves are characterized by a prefocal transmittance maximum (peak) followed by a postfocal transmittance minimum (valley) intensity. The transmission difference between peak and valley (ΔT_{p-v}) is written in terms of phase shift.

$$\Delta T_{p-v} = 0.406 (1-s)^{0.25} |\Delta \phi|$$

Linear transmittance aperture (S) is calculated using the relation
$$\mathbf{S} = \mathbf{1} - \exp\left(\frac{-2r_a^2}{\omega_a^2}\right)$$

where r_a is the radius of the aperture and ω_a is the beam radius at the aperture. The third-order nonlinear refractive index (n₂) of the crystal was calculated by following the relation.

$$n_2 = \Delta \phi / (K I_o L_{eff})$$

where I_0 is the intensity of the laser beam at the focus (Z = 0) and K = $2\pi/\lambda$ (λ is the wavelength of laser beam).

The effective thickness can be calculated using the relation

$$L_{eff} = [1-exp(-\alpha L)] / \alpha$$

where α is the linear absorption coefficient and L is the thickness of the

sample. The nonlinear absorption coefficient (β) can be calculated using the following relation

$$\beta \ = \frac{2\sqrt{2}\Delta T}{I_0 L_{eff}}$$

where ΔT is the one peak value at the open aperture Z-scan curve. The value of β will be negative for saturable absorption and positive for two photon absortion process. The real and imaginary parts of the third

order nonlinear optical suceptibility ($\chi^{(3)}$) are defined as Real part of $\chi^{(3)} = (10^4 \epsilon_0 \text{ c}^2 \text{ n}_0^2 \text{ n}_2) / \pi$ (esu) Imaginary part of $\chi^{(3)} = (10^2 \epsilon_0 \text{ c}^2 \text{ n}_0^2 \lambda \beta) / 4\pi^2$ (esu) Absolute value of $\chi^{(3)} = [\{\text{Real part of } \chi^{(3)}\}^2 + \{\text{Imaginary part of } \chi^{(3)}\}^2]^{1/2}$ (esu). Here ϵ_0 is the vacuum permitivity, n_o is the linear refractive index of the sample and c is the velocity of the light in vacuum. Using the above equations, nonlinear refractive index, third-order susceptibility and the nonlinear absorption coefficient of the crystals could be determined [19, 20]. Using a He-Ne laser and Z-scan experimental set up, the normalized transmittance was measured at different values of distance (Z) and it is to be mentioned that the thin crystalline sample was moved along the Z-direction and open and closed aperture Z-scan curved were drawn and the diagrams are shown in the figures 1-4. The estimated third order NLO parameters for the samples are given the table 1. It is noticed the nonlinear refractive index is negative because the closed aperture curves for the samples are showing peak followed by valley behavior. The normalized transmittance is observed to be more when lithium sulfate crystal is doped with rubidium chloride.

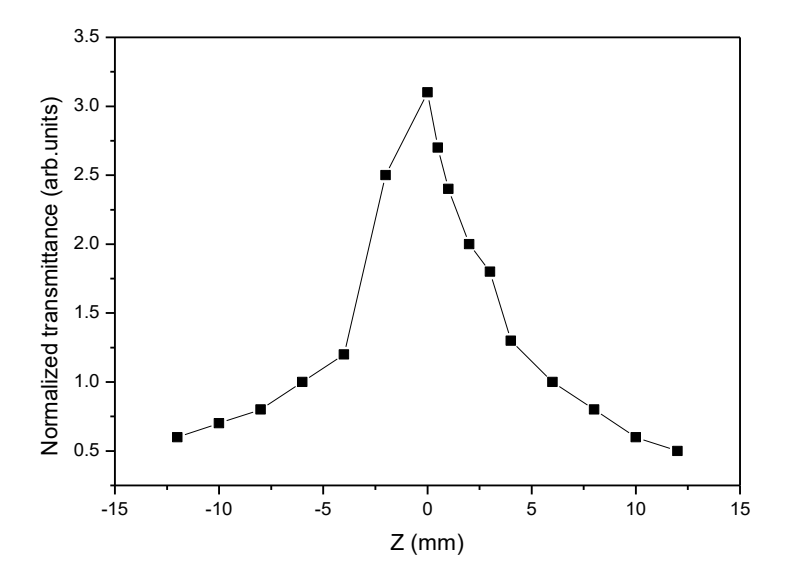


Figure 1: Open aperture Z-scan curve for lithium sulfate crystal

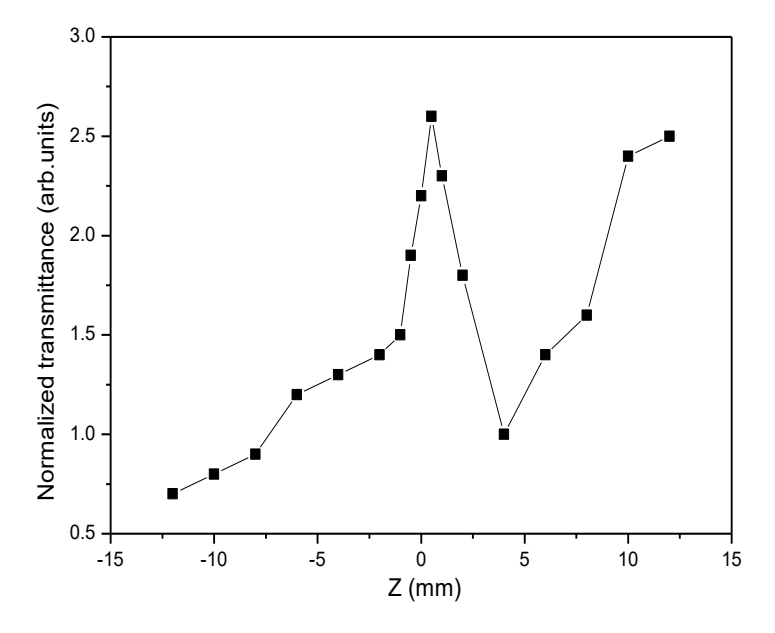


Figure 2: Closed aperture Z-scan curve for lithium sulfate crystal

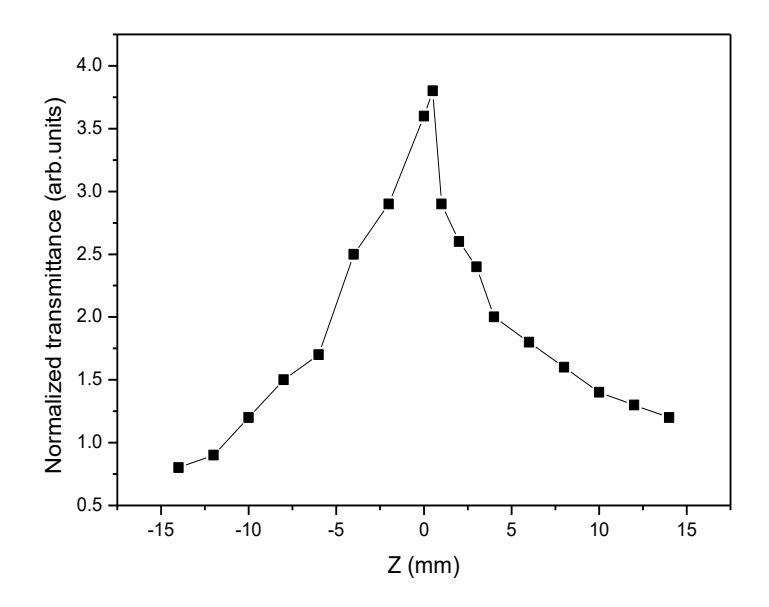


Figure 3: Open aperture Z-scan curve for rubidium chloride doped lithium sulfate crystal

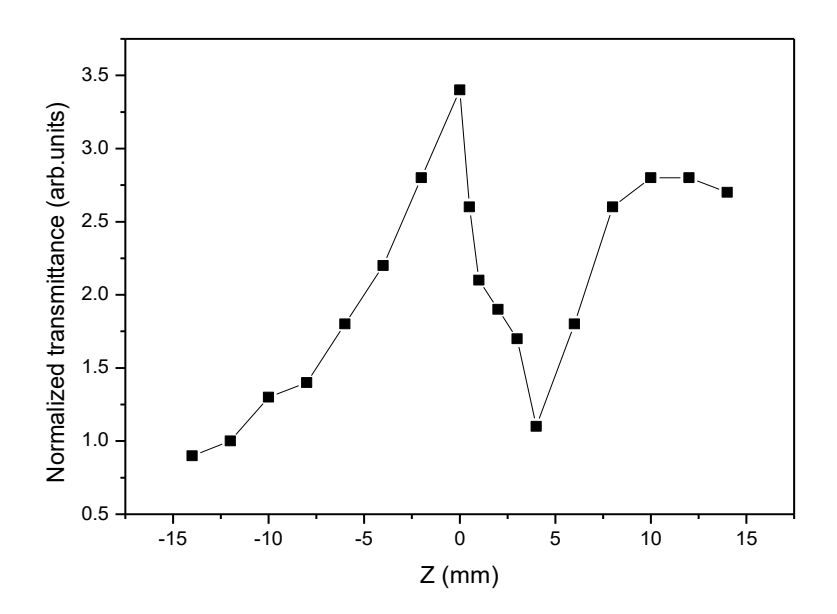


Figure 4: Closed aperture Z-scan curve for rubidium chloride doped lithium sulfate crystal Table 1: Third order NLO parameters of undoped and rubidium chloride doped lithium sulfate crystals

Sample	Nonlinear refractive index (n ₂) x 10 ⁻¹¹	Nonlinear absorption coefficient (β) x 10 ⁻⁴	Third order nonlinear susceptibility ($\chi^{(3)}$)
	(m^2/W)	(m/W)	$\times 10^{-7} (esu)$
Undoped lithium sulfate crystal	-4.724	3.783	1.894
Rubidium chloride doped lithium sulfate crystal	-5.682	2.986	2.037

6. Dielectric Analysis:

Dielectric analysis gives the information regarding the dielectric phenomena that arises from the contributions of different polarizations namely electronic, ionic, orientational and space charge polarizations that are developed in the material when it is subjected to the varying electric field. Space charge polarization is active at low frequencies upto 10^3 Hz and orientational polarization is active in frequency region of 10^3 Hz to 10^6 Hz. The ionic and electronic polarizations are active beyond 10^6 Hz [21, 22]. The dielectric characteristics of

the material are important to know the transport phenomena and the lattice dynamics in the crystal. Dielectric properties are correlated with electro-optic properties of the crystals. The sample was electroded on either side with graphite coating to make it behave like a parallel plate capacitor. Using NETZSCH STA 409 C/CD LCR meter, the capacitance and dielectric loss (tan δ) were measured at the frequency of 1 kHz, 10 kHz and 1 MHz at various temperatures. The dielectric permittivity of the crystal was calculated using the relation $\epsilon_r = C/C_0$ where C is the capacitance of the crystal and Co is the capacitance of the same dimension of air. Figures 5-6 show the variations of dielectric constant (ϵ_r) with temperature at different frequencies for undoped lithium sulphate monohydrate crystal and rubidium sulphate doped lithium sulphate crystal. The variations of dielectric loss with temperature at different frequencies for the samples are presented in the figures 7-8. The results indicate that the dielectric parameters such as dielectric constant and loss factor increase with increase of temperature but these values are observed to be decreasing with increase of frequency. The higher values of dielectric parameters at low frequency region are due to space charge polarization. The low value of dielectric loss (tan δ) indicates that the grown crystals are of high quality. Low dielectric materials are needed for microelectronics industry. Lowering the dielectric constant value of interlayer dielectric decreases the RC delay, lowers power consumption, and reduces cross-talk between nearby connects [23,24]. The dielectric parameters are observed to be increasing when lithium sulphate crystals are doped with rubidium chloride. AC conductivity of the samples was determined using the relation $\sigma_{ac} = 2\pi f \epsilon_o \epsilon_r \tan \delta$ where f is the frequency of ac signal, ϵ_o is the permittivity of free space, ϵ_r is the dielectric constant and tan δ is the dielectric loss of the sample. The plots of AC conductivity versus temperature at different frequencies are shown in the figures 9-10. From the results, it is noticed that the conductivity increases with increase of temperature indicating the insulating nature of the grown crystals and there is an increasing nature of the dielectric parameters when lithium sulphate crystals are doped with rubidium chloride.

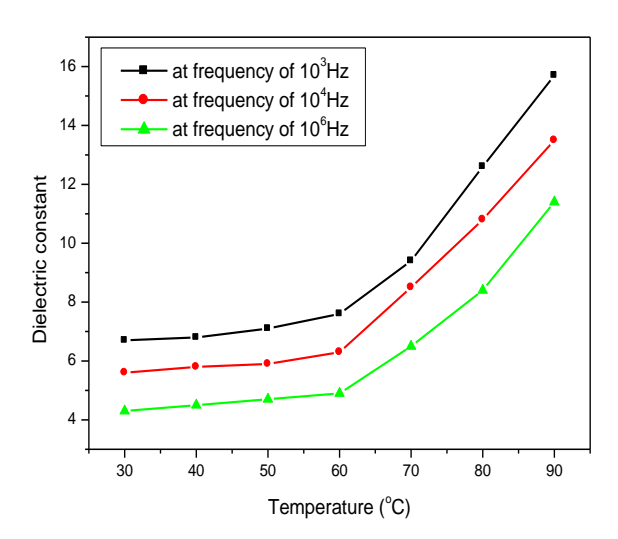


Figure 5: Temperature dependence of dielectric constant for undoped lithium sulfate crystal at different frequencies

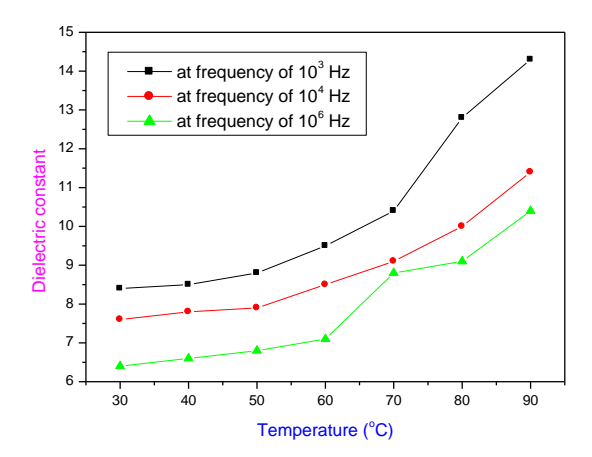


Figure 6: Temperature dependence of dielectric constant for rubidium chloride doped lithium sulfate crystal at different frequencies

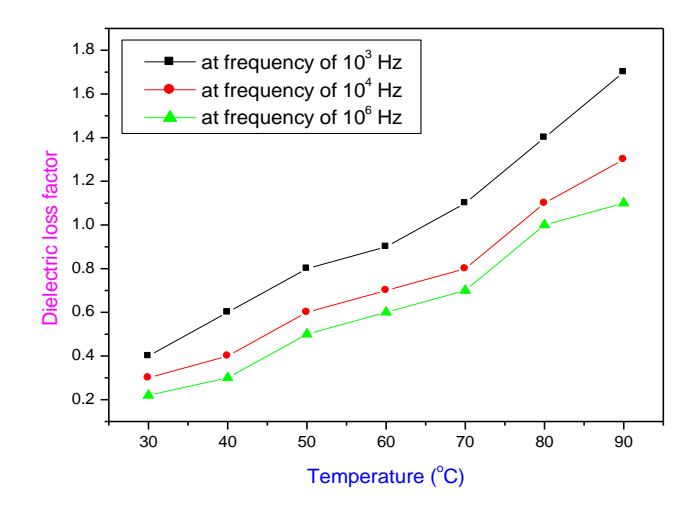


Figure 7: Plots of variations of dielectric loss factor with temperature for undoped lithium sulfate monohydrate crystal at different frequencies

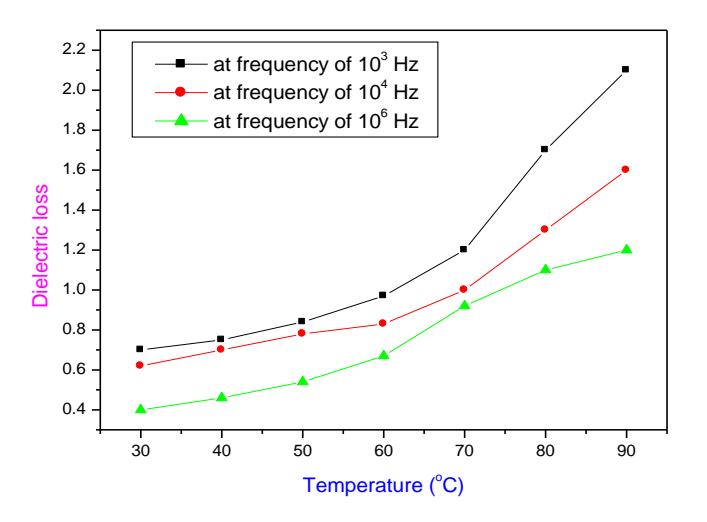


Figure 8: Plots of variations of dielectric loss factor with temperature for rubidium chloride doped lithium sulfate crystal at different frequencies

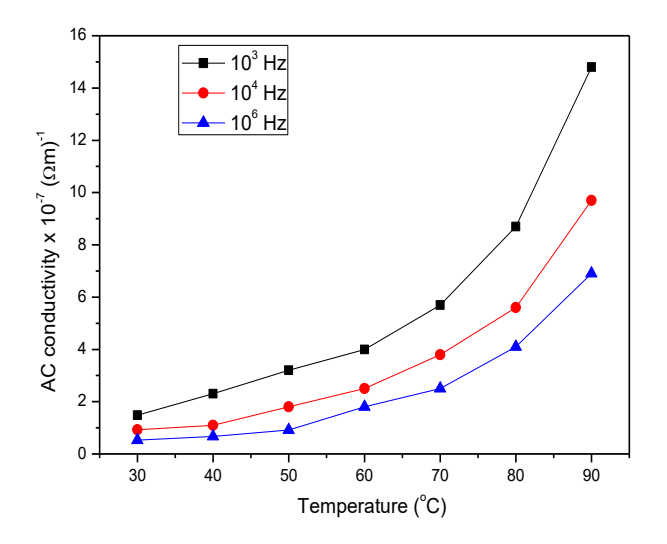


Figure 9: Plots of AC conductivity versus temperature for undoped lithium sulfate crystal at different frequencies

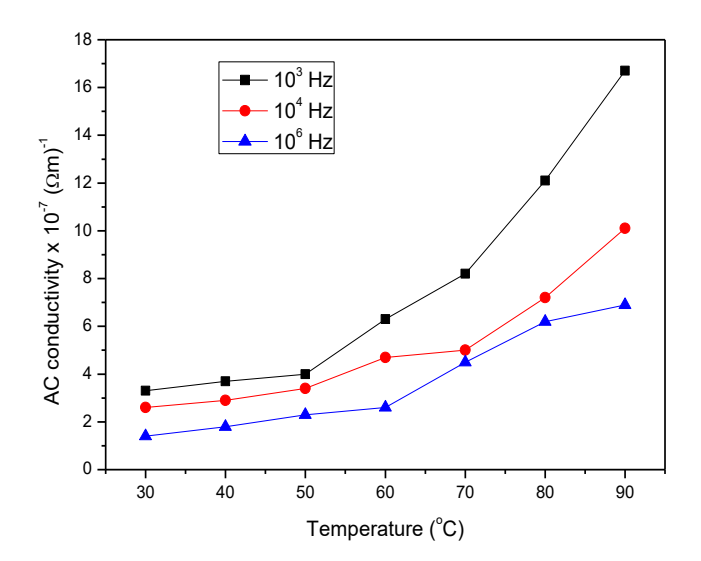


Figure 10: Plots of AC conductivity versus temperature for rubidium chloride doped lithium sulfate crystal at different frequencies

7. Conclusions:

Slow evaporation method was adopted to grow the crystals of undoped and rubidium chloride doped lithium sulfate and the crystal structure was found to be monoclinic by single crystal XRD method. Kurtz powder technique was used to find the relative second harmonic generation efficiency. Third order NLO parameters like nonlinear refractive index, nonlinear absorption coefficient and nonlinear susceptibility were determined by Z-scan technique. It is observed that the third order NLO parameters are enhanced when lithium sulfate crystals are doped with rubidium chloride. The dielectric constant and loss factor were estimated at different temperatures and the values of AC conductivity for the samples were determined and the conductivity is found to be increased when lithium sulfate crystals are doped with rubidium chloride.

8. Acknowledgement:

The authors are grateful to the staff members of NIT, Trichy, Crescent Engineering College, Chennai and S.T. Hindu College, Nagercoil for having helped in taking the research data for the samples.

9. References:

- 1. A. S. J. Luciarose, P. Selvarajan, P. Perumal, Physica B, 406 (2011) 412-417.
- 2. A. Puhal Raj, C.Ramachandra Raja, Spectrochimica Acta Part A, 97 (2012) 83-87.
- 3. V. G. Dmitriev, Gurzadyan, G. Gagik, Nikogosyan, N. David, Handbook of Nonlinear Optical Crystals, Springer, London (1999).
- 4. R. R. Levitskii, I. R. Zachek, A. S. Vdovych, S. I. Sorokov, Condens. Matter Phys. 12, (2009) 75–119.
- 5. M. E. Hagerman, K. R. Poeppelmeier, Chem. Mater. 7 (1995) 602–621.
- 6. E. M. Brody, H.Z. Cummins, Phys. Rev. Lett. 21 (1968) 1263–1266
- 7. A. Clearfield, D. S. Thakur, Appl. Catal. A 26 (1986) 1–26.
- 8. H. Onoda, K. Tange, I. Tanaka, J. Mater. Sci. 43 (2008) 5483–5488.
- 9. P. Groth, Chemische Krystallographie, Leipzig, Germany, 1908.
- 10. W. Ackermann, J. Phys. C: Solid State Phys. 46 (1912) 197.
- 11. S. B. Lang, Phys. Rev. B: Condens. Matter 4 (1971) 3603.
- 12. H. G. Smith, S. W. Peterson et al. J. Chem. Phys. 48(1968)5561
- 13. A. C. Larson, L. Helmholtz, J. Chem. Phys. 22(1954) 2049.
- 14. G. E. Ziegler, Z. Krist. 89(1934) 456.
- 15. P. Manimekalai, P. Selvarajan, Int. J. Appl. Adv. Sci. Res. 2 (2017) 331-339.
- 16. S. K. Kurtz, T. T. Perry, J. Appl. Phy. 39 (1968) 3798.
- 17. N. J. Dovichi, J. M. Harris, Anal. Chem 51 (1979)728–731.
- 18. S. Leela, K. Ramamurthi, G. Bhagavannarayana, Spectrochim. Acta Part A 74 (2009)78–83.
- 19. V. Subhashini, S. Ponnusamy, C. Muthamizhchelvan, J.Cryst.Growth363 (2013)211–219.
- 20. E. M. Van Stryland, M. Sheik-Bahae, M. G. Kuzyk, C. W. Dirk, Marcel DekkerInc. 998,655-692.
- 21. J. C. Anderson, Dielectrics, first ed., Wiley, London, 1964.
- 22. S. Suresh, Mater. Phys. Mech. 14 (2012) 145-151.
- 23. I. Bunget, M. Popescu, Physics of Solid Dielectrics, Elsevier, New York (1984).
- 24. C. Krishnan, P. Selvarajan, T. H. Freeda, C. K. Mahadevan, Physica B, 404 (2009) 289.